Controlling Floor Vibration with Active and Passive Devices

Linda M. Hanagan[1], Thomas M. Murray[2], and Kamal Premaratne[3]

ABSTRACT—This paper reviews research, conducted by the authors over the last decade, pertaining to the control of excessive floor vibration using active and passive devices. The active device studied uses a proof-mass actuator to deliver the control force to the floor system. Effectiveness and stability characteristics for a single-input/single-output (SISO) control scheme, using velocity feedback, are explored. The SISO system is shown to increase damping to 40% of critical on an experimental floor when amplitudes remain in the linear range. When implemented on two in-place floors, at least a 70% reduction in vibration amplitudes due to walking was observed. Next, the benefits of expanding to a practical single-input/multi-output (SIMO) control system are identified. Additionally, techniques to optimize the SIMO scheme are presented. Because of the stability characteristics of the controlled system, the improvement noted for the SIMO scheme is most dramatic for floors with fundamental frequencies near the natural frequency of the actuator. In a 2 Hz floor example, a SIMO control scheme provided seven times more reduction than that of the SISO system. The passive device research focuses on the experimental implementation of tuned mass dampers (TMDs) to control floor vibration. Two different configurations are explored. The uniqueness of the first device is that liquid filled bladders are used to provide an economical damping mechanism. When implemented on an office floor, a significant improvement of walking vibration levels was observed. Satisfaction with the repair was noted from the occupants. The second device utilizes a configuration that has great flexibility in the field, thus allowing for more economical mass production. Using two TMDs, a significant reduction of response was noted for the 5 and 6 Hz modes. Research to improve these active and passive strategies continues and will be reported as significant results are achieved.

KEYWORDS: floor vibration, active control, tuned mass damper, liquid damper, proof-mass actuator

1. Introduction

Humans are very sensitive vibration sensors. Floor motion with displacements as small as 1 mm can be annoying to building occupants. Human sensitivity is dependent on a large number of factors including surrounding activities and body position. Sensitivity increases with decreasing environmental noise; for instance, an occupant of a residence is more sensitive than a shopper in a busy shopping mall (Murray et al., 1997). Weight lifters on floors being used for aerobic exercising are more sensitive than people waiting to exercise. Humans seem to be more sensitive when sitting as compared to standing. With all of these factors involved, it is very difficult to develop criteria that result in reasonably economical floor framing systems while accurately predicting the human response over a wide range of sensitivity and floor framing parameters.

Vibration sensitivity criteria, pertinent to evaluating floor systems, have been under development for almost the entire twentieth century (Reiher and Meister, 1931; Lenzen, 1966; Wiss and Parmelee, 1974; CSA, 1989; Wyatt, 1989; Allen, 1990; Murray, 1991; ISO, 1992; Allen and Murray, 1993; Murray et al., 1997). Different vibration limits are required for floor systems used for normal living and business activity than those used for more vigorous activity such as lively dancing or aerobic exercising. The former generally requires the estimation of damping for structural (i.e. beams, slabs, deck) and non-structural (i.e. partitions, file cabinets, people) elements, which is difficult to say the least. Since no significant study has been made of damping sources and magnitudes, only general guidelines are available. Criteria for floors subject to rhythmic activities require an accurate prediction of the fundamental frequency. Because of the varied interaction of the framing components, composite, partially composite, and non-composite behavior, an accurate design prediction of the floor frequency is difficult. To make matters more difficult, certain activities require floor systems to have frequencies above 7–9 Hz, thus requiring small span-to-depth ratios for economical designs. Recent experience has shown that the use of trusses, such as joists and joist girders, for these systems may result in a significantly lower frequency than is predicted by usual methods (Kitterman and Murray, 1994; Band and Murray, 1996).

The consequence of the above is that floors are sometimes constructed and later found to vibrate at levels that are annoying to building occupants. Correcting these floors is extremely difficult and can be expensive. Structural changes, such as the addition of columns or increasing beam or girder sections by cover plating are usually cost prohibitive or impractical to the building function. Additionally, these retrofits must often be done in the occupied building; this adds significantly to the cost. An alternative approach is to control the floor motion using either passive or active systems. Research pertaining to these alternatives is presented in this paper.

[1] *Assistant Professor, Architectural Engineering Department, The Pennsylvania State University.*
[2] *Professor, Charles Edward Via, Jr. Department of Civil and Environmental Engineering, Virginia Polytechnic Institute and State University.*
[3] *Associate Professor, Department of Electrical and Computer Engineering, University of Miami.*

The Shock and Vibration Digest, Vol. 35, No. 5, September 2003 347–365

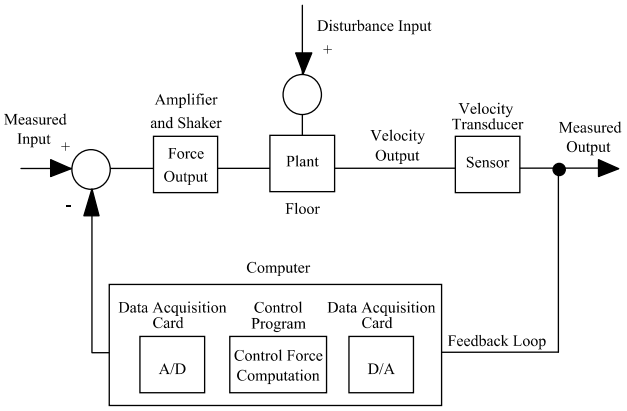

Figure 1. Block diagram of SISO control setup.

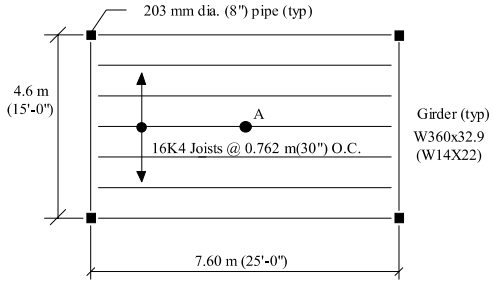

Figure 2. Plan and section of experimental test floor.

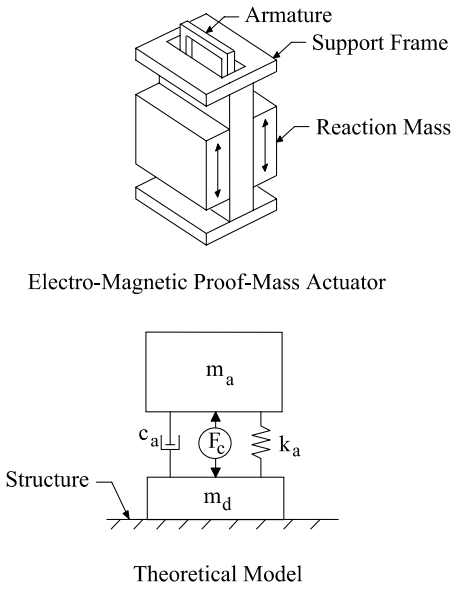

Figure 3. Illustration and theoretical model of control actuator.

2. Single-Input/Single-Output Control Research

Research on actively controlling floor vibration began with the investigation of a single-input/single-output (SISO) control scheme. In this scheme, the measured movement of the floor system is utilized in a feedback configuration to supply a control force that results in a reduction of vibration levels. To supply a control force, an effective and readily available mechanism is an electromagnetic proof-mass actuator (Preumont, 2002, p. 38). Such a device relies on the inertial effect of a moving mass to deliver the necessary control force to the structure. A piezoelectric velocity sensor is used in a collocated rate feedback control algorithm (Preumont, 2002, p. 93) that is implemented using a personal computer equipped with a data acquisition card possessing both input and output channels. A schematic diagram illustrating the SISO control setup is shown in Figure 1. The goal of the control scheme is to add damping to the floor system, thus improving the floor system response with respect to human perception. In the following sections, the analytical and experimental research for this SISO control strategy is described. Much of this research has been previously reported in Hanagan (1994), Hanagan and Murray (1994, 1995a, 1995b, 1997, 1998), Rottmann and Murray (1996), Saaid et al. (1996).

2.1. Experimental Test Floor

A full-scale test floor was designed and constructed for use in the experimental implementation of passive and active structural control described in this paper. To resemble an actual problem floor, the test floor was designed with certain framing characteristics. Complaints of annoying floor vibrations have been commonly reported in office-type occupancies constructed of steel joist framing members supporting thin concrete slabs, even when they have been properly designed for strength and static live load deflection requirements. The test floor is, therefore, of this construction type and was designed for the strength required by an office occupancy.

A joist span of 7.60 m (25 ft) with joist spacing of 0.762 m (30 in), common dimensions for this construction type, was selected. The joists (16K4) are 406 mm deep, lightweight, steel trusses. The girder span was limited to 4.6 m (15 ft) because of laboratory space limitations. The lightweight concrete slab, supported by 25 mm (1in) light gage metal deck, has a total thickness of 89 mm (3.5 in). The girders are supported by 203 mm (8 in) diameter pipe columns welded to base plates that are anchor bolted to the concrete laboratory floor. A plan of the test floor is shown in Figure 2. Both experimental measurements and subjective human evaluation of the constructed floor described the floor response to walking excitation as extremely perceptible and, therefore, unacceptable.

2.2. Control System Hardware

An APS Dynamics Electro-Seis 400 electro-dynamic shaker including the reaction mass assembly (Figure 3) was selected with a specified maximum force output of 445 N (100 lb) and a stroke limitation of 76.2 mm (±3 in) to provide the control force. This device, as configured, can be generically referred to as a proof-mass actuator. The APS shaker, measuring 24W × 21D × 52H cm^3, can be easily mounted inside most ceiling cavities. A custom designed power amplifier delivers the necessary current to drive the shaker. Because the actuator relies on an inertial mass supported

Table 1. Actuator and sensor parameters.

Parameter	Quantity
Actuator force, F_c	267 N V^{-1}
Reaction mass, m_a	30.4 kg
Parasitic mass, m_p	74.0 kg
Actuator spring stiffness, k_a	2700 N m^{-1}
Actuator damping, c_a	165 N $(m\ s^{-1})^{-1}$
Sensor filter frequency, ω_s	22.0 rad s^{-1}
Sensor filter damping ratio, ζ_s	0.55

by elastic bands to generate the output force, additional dynamics are introduced into the controlled system. These dynamics, through actuator/structure interaction, can produce instabilities in a control system which would otherwise be stable (Balas, 1979). This concept will be expanded and evaluated in a later section.

The dynamic behavior of the actuator can be closely described by a linear second-order model (Zimmerman and Inman, 1990) as illustrated in Figure 3. The second-order model of the shaker possesses discrete masses, m_a and m_d, which represent the reaction (active) mass and the parasitic mass (support frame, etc.), respectively. The spring stiffness, k_a, is supplied by the suspension system consisting of elastic bands attached to the support frame and the reaction mass. The internal damping, due to internal coil properties and friction, is represented by c_a and is assumed to be viscous. The input voltage can be reasonably assumed to have a linear relationship with the force generated in the electromagnetic coil (Premont, 2002, p. 39), F_c, as noted in Figure 3. The linear relationship and the relevant actuator parameters were experimentally determined and are defined in Table 1.

A PCB/IMI V0326A01 piezoelectric velocity sensor with a model 482B11 signal conditioner is used in a feedback control scheme. The manufacturer lists a 2.5 to 2500 Hz bandwidth of operation. This sensor is actually a piezoelectric accelerometer with an integrator circuit whereby the lower limit on the bandwidth is a result of the integrator circuit properties. Because the frequency bandwidth for the controller operation extends below the lower limit of the sensor, the integrator circuit properties cannot be neglected. The integrator circuit can be expressed as a filter whose dynamic properties can be determined experimentally. The Laplace transform of the estimated filter is as follows

$$\text{filter} = \frac{s}{s^2 + 2\zeta_s \omega_s s + \omega_s^2} \tag{1}$$

where s is the complex variable, ω_s is the circular natural frequency of the second-order filter, and ζ_s is the damping ratio of sensor filter. These properties are defined in Table 1. This filter, comprised of electronic elements, closely emulates the magnitude and phase shift of an ideal integrator at frequencies above 2 Hz.

2.3. State-Space Model

In this section, we describe the formulation of the SISO state-space model used to study the uncontrolled and controlled floor system. This type of model is particularly convenient for two reasons. First, it provides easy transition between modal and spatial response variables. Secondly, control system analysis and design software often requires that the system properties be expressed in this form (MATLAB, 1998).

2.3.1. Floor Model

To design and study a control scheme for reducing the excessive vibration levels, an analytical model of the experimental floor system was developed. The behavior of the distributed-parameter floor system was simulated mathematically using a lumped-parameter model possessing "*m*" modal (normal) and "*n*" spatial coordinates. This type of model is particularly convenient because the modal parameters can be determined using finite element analysis and/or experimental modal analysis. The general form for this type of model is

$$M^* \cdot \ddot{Z} + C^* \cdot \dot{Z} + K^* \cdot Z = \Phi^T \cdot F(t) \tag{2}$$

$$Y = \Phi \cdot Z \tag{3}$$

where $\ddot{Z}, \dot{Z}, Z$ are the modal acceleration, velocity, and displacement vectors, respectively, each containing m elements; $\dot{Y}, Y$ are the spatial velocity and displacement vectors, respectively, each containing n elements; and $F(t)$ is the input force vector containing n elements.

$$\Phi = \begin{bmatrix} \Phi_{11} & \Phi_{12} & \cdots & \Phi_{1m} \\ \Phi_{21} & \Phi_{22} & \cdots & \Phi_{2m} \\ \vdots & \vdots & \ddots & \vdots \\ \Phi_{n1} & \Phi_{n2} & \cdots & \Phi_{nm} \end{bmatrix} = \begin{bmatrix} \Phi_1 \\ \Phi_2 \\ \vdots \\ \Phi_n \end{bmatrix} = \begin{matrix} \text{modal} \\ \text{transformation} \\ \text{matrix} \end{matrix}; \tag{4}$$

$$M^* = \begin{bmatrix} 1 & 0 & \cdots & 0 \\ 0 & 1 & & 0 \\ \vdots & \vdots & \ddots & \\ 0 & 0 & & 1 \end{bmatrix}_{m \times m} = \begin{matrix} \text{modal} \\ \text{mass} \\ \text{matrix} \end{matrix}; \tag{5}$$

$$C^* = \begin{bmatrix} 2\zeta_1 \omega_1 & 0 & \cdots & 0 \\ 0 & 2\zeta_2 \omega_2 & & 0 \\ \vdots & & \ddots & \\ 0 & 0 & & 2\zeta_m \omega_m \end{bmatrix} = \begin{matrix} \text{modal} \\ \text{damping} \\ \text{matrix} \end{matrix} \tag{6}$$

where ζ_i is the modal damping coefficient for ith mode and ω_i is the circular natural frequency for the ith mode.

$$K^* = \begin{bmatrix} \omega_1^2 & 0 & \cdots & 0 \\ 0 & \omega_2^2 & & 0 \\ \vdots & & \ddots & \\ 0 & 0 & & \omega_m^2 \end{bmatrix} = \begin{matrix} \text{modal} \\ \text{stiffness} \\ \text{matrix} \end{matrix}. \tag{7}$$

From inspection of the above equations, the parameters required in the analysis of a specific floor system are the circular natural frequencies, the modal damping coefficients, and the modal transformation matrix, for a prescribed number of vibration modes and spatial coordinates. The number of vibration modes selected to accurately model the dynamic response of the floor was a matter of judgment affected by several factors. Research by Pernica (1990) quantifies

Table 2. Measured natural frequencies and damping ratios for experimental test floor.

	Frequency (Hz)	Damping ratio (ζ_i)
Mode 1	7.3	0.0050
Mode 2	9.4	0.0085
Mode 3	16.5	0.0085
Mode 4	16.9	0.0050
Mode 5	26.5	0.0055

dynamic load factors for walking and other rhythmic activities. These dynamic load factors were experimentally determined by measuring the forces created by these activities. Walking was shown to produce an excitation having frequency content at harmonic multiples of the step frequency. The Fourier amplitude at each harmonic decreases as the multiple of the step frequency increases. The step frequencies studied for walking were between 1 and 3 Hz. The most comfortable pacing frequencies were observed between 1.6 and 2.2 Hz. Dynamic load factors, based on the Fourier amplitudes, were 0.56, 0.28, 0.16, and 0.09 for the first four harmonics of the step frequency. Because of this relationship, modes of vibration with frequencies above that of the fourth harmonic of walking do not contribute significantly to the response of a floor system excited by walking. Preliminary testing confirmed that the lower-frequency modes of vibration dominated the dynamic response when the floor was subjected to walking excitation. Therefore, only the modes of vibration with natural frequencies less than 30 Hz are included in the analytical model.

Because ω_i and ζ_i are global parameters (i.e., not unique to a single floor location), they can be determined from relatively few experimental measurements. A series of experimental tests was conducted to determine the natural frequency and damping ratios for the modes of vibration with natural frequencies less than 30 Hz. Using experimental velocity output and force input measurements, frequency response functions (FRFs) (McConnel, 1995, p. 73) were computed for several locations on the test floor. Sharp peaks on the magnitude versus frequency plots of the FRFs occur at the floor system's natural frequencies. The modal damping ratios, ζ_i, were also determined from the FRF plots using the quadrature peak picking method as described by Inman (1994, p. 379). Five distinct modes of vibration were identified for frequencies less than 30 Hz. The natural frequencies and damping ratios experimentally determined for these five modes are listed in Table 2.

The mode shapes corresponding to these natural frequencies could also be determined through experimental testing using modal analysis. Because extensive testing hardware is necessary for such an analysis, a finite element model was alternatively utilized to determine the modal transformation matrix, Φ, for the floor system. In a commercially available structural analysis software package, beam and plate elements, configured in a single plane, were used to model the steel framing members and the concrete slab, respectively. This type of model has proven successful in predicting dynamic floor behavior (Morley and Murray, 1993.) Spring supports were used at the four corners to include the measured displacements at these locations. A mesh size of 0.762 × 0.762 m^2 (30 × 30 in^2) produced

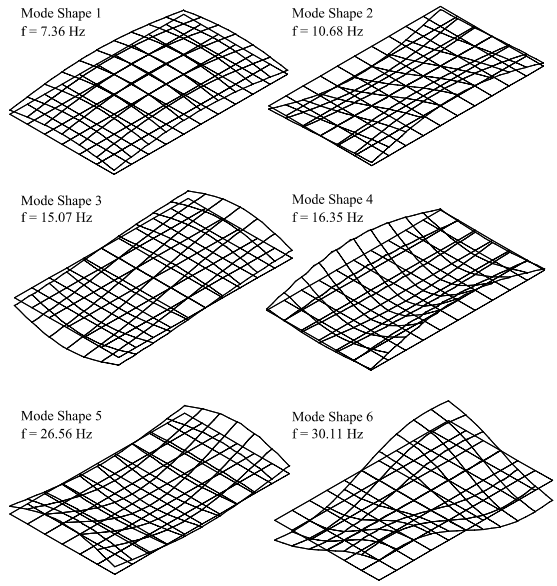

Figure 4. Mode shapes from finite element analysis.

77 spatial coordinates in an 11 × 7 node grid. An analysis was also performed using a smaller mesh size of 0.381 × 0.381 m^2 (15 × 15 in^2); however, no significant change was noted in the dynamic response due to this refinement. Therefore, the larger mesh size was considered sufficiently refined for this study. Figure 4 shows the frequencies and mode shapes corresponding to the first six modes, as computed from the finite element model.

2.3.2. Control Algorithm

Any dynamic system controlled using "feedback" has two common characteristics: a means of monitoring behavior and a means to correct unwanted behavior (Friedland, 1986, p. 2). When a disturbance is introduced to a floor system as a result of human activities such as walking, jumping, or dancing, feedback control can be implemented to bring a vibrating floor back to a stationary equilibrium position more quickly. Many factors must be considered when designing a controller for a complex structure. For application in floor systems, the controller must be robust to system uncertainties and changes, otherwise the control system may become ineffective or produce undesirable results. As noted in the Introduction, an objectionable floor system can often be improved by adding damping to the structure. A commonly utilized control law, direct velocity feedback (collocated rate feedback; Franklin et al., 1986), was selected for experimental implementation because of its ability to add damping to the system while providing the necessary robustness (Balas, 1979). In this application, velocity sensor outputs are multiplied by gains and fed back to collocated force actuators. For a single actuator/sensor pair, as is the case in this research, this control law is expressed as

$$F_a = -g \cdot \dot{y}_s \tag{8}$$

where g is the control gain, $\dot{y}_s$ is the collocated velocity sensor measurement, and F_a is the force between the reaction mass of the actuator and the floor system as shown in Figure 3. The merit of this method is that the effect on the

unmodeled higher frequency modes is always stabilizing. In fact, in the absence of actuator and sensor dynamics, direct velocity feedback is unconditionally stable (Balas, 1979). The stability characteristics, with the inclusion of sensor and actuator dynamics, are discussed later in this paper.

2.3.3. System Model

The model of the floor system developed earlier (equations (2)–(7)) can be expanded to include the dynamics of the control actuator. The actuator adds an additional degree of freedom to the system, resulting in the following expansion of equation (2)

$$\begin{bmatrix} M^* + \Phi_a^T \cdot m_d \cdot \Phi_a & 0 \\ 0 & m_a \end{bmatrix} \begin{Bmatrix} \ddot{Z} \\ \ddot{z}_{m+1} \end{Bmatrix} + \begin{bmatrix} C^* + \Phi_a^T \cdot c_a \cdot \Phi_a & -c_a \cdot \Phi_a^T \\ -c_a \cdot \Phi_a & c_a \end{bmatrix} \begin{Bmatrix} \dot{Z} \\ \dot{z}_{m+1} \end{Bmatrix} + \begin{bmatrix} K^* + \Phi_a^T \cdot k_a \cdot \Phi_a & -k_a \cdot \Phi_a^T \\ -k_a \cdot \Phi_a & k_a \end{bmatrix} \begin{Bmatrix} Z \\ z_{m+1} \end{Bmatrix} = \begin{Bmatrix} \Phi^T \cdot F(t) \\ 0 \end{Bmatrix} + \begin{bmatrix} \Phi_a^T \\ -1 \end{bmatrix} \cdot F_a(t) \tag{9}$$

where

$$\Phi_a = \begin{bmatrix} \Phi_{a1} & \Phi_{a2} & \cdots & \Phi_{am} \end{bmatrix} \tag{10}$$

is the coordinate transformation matrix at spatial coordinate a, row a from the modal transformation vector defined in equation (4). Coordinate a is the node selected as the actuator location on the floor model. $\ddot{z}_{m+1}, \dot{z}_{m+1}, z_{m+1}$ are the actuator mass acceleration, velocity, and displacement, respectively. The remaining parameters in the equation above are defined in Sections 2.3.1 and 2.3.2.

The sensor dynamics must also be added to a particular output coordinate. In the case of collocated velocity feedback the sensor coordinate is defined by Φ_a. The resulting equations are

$$\begin{bmatrix} M^* + \Phi_a^T \cdot m_d \cdot \Phi_a & 0 & 0 \\ 0 & m_a & 0 \\ -\Phi_s & 0 & 1 \end{bmatrix} \begin{Bmatrix} \ddot{Z} \\ \ddot{z}_{m+1} \\ \ddot{z}_s \end{Bmatrix} + \begin{bmatrix} C^* + \Phi_a^T \cdot c_a \cdot \Phi_a & -c_a \cdot \Phi_a^T & 0 \\ -c_a \cdot \Phi_a & c_a & 0 \\ 0 & 0 & 2\zeta_s \omega_s \end{bmatrix} \begin{Bmatrix} \dot{Z} \\ \dot{z}_{m+1} \\ \dot{z}_s \end{Bmatrix} + \begin{bmatrix} K^* + \Phi_a^T \cdot k_a \cdot \Phi_a & -k_a \cdot \Phi_a^T & 0 \\ -k_a \cdot \Phi_a & k_a & 0 \\ 0 & 0 & \omega_s^2 \end{bmatrix} \begin{Bmatrix} Z \\ z_{m+1} \\ z_s \end{Bmatrix} = \begin{Bmatrix} \Phi^T \cdot F(t) \\ 0 \\ 0 \end{Bmatrix} + \begin{bmatrix} \Phi_a^T \\ -1 \\ 0 \end{bmatrix} \cdot F_a(t). \tag{11}$$

The system of equations above can be expressed in the state space by defining the state-space variables in the general form:

$$\dot{X} = AX + BU$$

$$Y = CX + DU. \tag{12}$$

The variables of the state space are as follows.

$$X^T = \{x_1 \quad x_2 \quad \cdots \quad x_{2m+4}\} = \{z_1 \quad \cdots \quad z_{m+1} \quad z_s \quad \dot{z}_1 \quad \cdots \quad \dot{z}_{m+1} \quad \dot{z}_s\} \tag{13}$$

is the state variable vector.

$$Y^T = \{y_1 \quad y_2 \quad \cdots \quad y_n \quad y_a \quad \dot{y}_1 \quad \dot{y}_2 \quad \cdots \quad \dot{y}_n \quad \dot{y}_a \quad \dot{y}_s\} \tag{14}$$

is the output vector where y_a and $\dot{y}_a$ are the actuator displacement and velocity, respectively and $\dot{y}_s$ is the velocity sensor output.

$$A = \begin{bmatrix} 0_{M\times M} & I_{M\times M} \\ -\dfrac{K_s}{M_s} & -\dfrac{C_s}{M_s} \end{bmatrix} \tag{15}$$

where M is the number of modeled floor modes plus 2 and K_s, C_s, and M_s are the system stiffness, damping, and mass matrices defined in equation (11).

$$U = \begin{Bmatrix} F(t) \\ F_a(t) \end{Bmatrix} \tag{16}$$

is the input vector where $F(t)$ is the disturbance force and $F_c(t)$ is the control force.

$$B = \begin{bmatrix} 0_{M\times 1} & 0_{M\times 1} \\ \dfrac{B_d}{M_s} & \dfrac{B_c}{M_s} \end{bmatrix} \tag{17}$$

where

$$B_d^T = \begin{bmatrix} \Phi^T & 0 & 0 \end{bmatrix} \tag{18}$$

and

$$B_c^T = \begin{bmatrix} \Phi_a^T & -1 & 0 \end{bmatrix}. \tag{19}$$

$$C = \begin{bmatrix} \Phi & 0_{n\times 1} & 0_{n\times 1} & 0_{n\times m} & 0_{n\times 1} & 0_{n\times 1} \\ 0_{1\times m} & 1 & 0 & 0_{1\times m} & & \\ 0_{n\times m} & 0_{n\times 1} & 0_{n\times 1} & \Phi & 0_{n\times 1} & 0_{n\times 1} \\ 0_{1\times m} & 0 & 0 & 0_{1\times m} & 1 & 0 \\ 0_{1\times m} & 0 & 0 & 0_{1\times m} & 0 & 1 \end{bmatrix} \tag{20}$$

$$D = \begin{bmatrix} 0_{1\times n} & 0 \end{bmatrix}. \tag{21}$$

2.4. Root Locus Study

The analytical model developed in the previous section can be used to study the effectiveness and stability of the control system. In a SISO control scheme, classical control techniques are very helpful in understanding the system

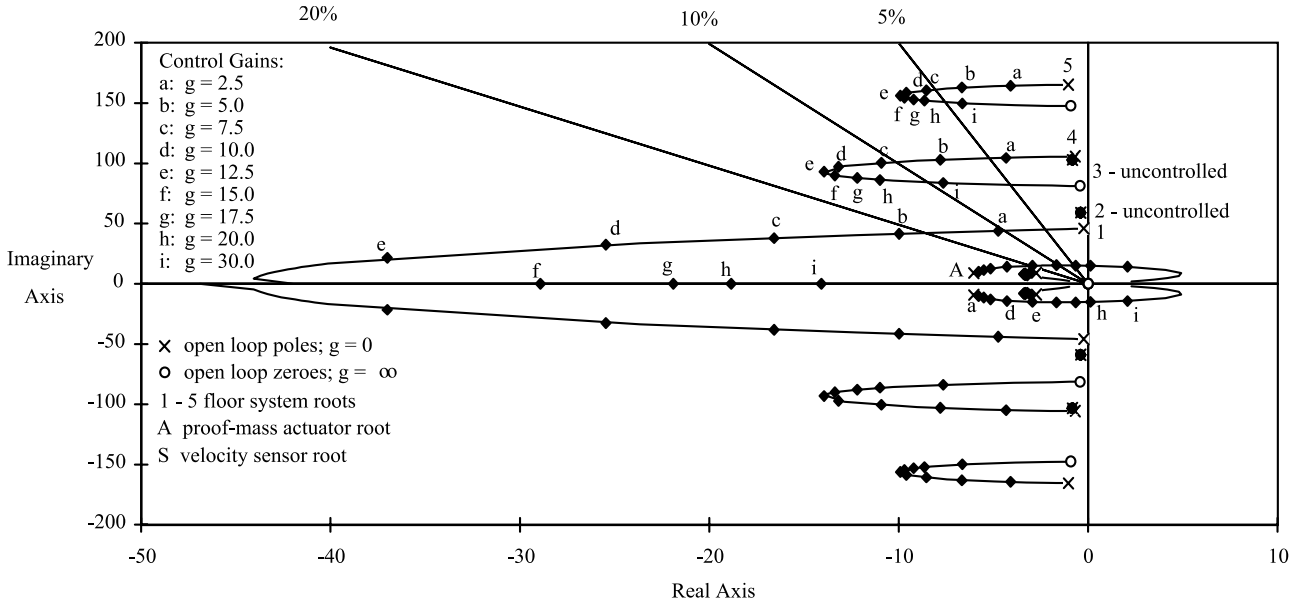

Figure 5. Root locus diagram for collocated velocity feedback.

behavior. The root locus (Van de Vegte, 1990), in effect, maps the complex linear system roots for control gains (g in equation (8)) ranging from zero to infinity. The first mode of vibration was selected as the main target of control. To control this mode, the actuator and velocity sensor are placed at the center of the test floor, noted point A in Figure 2 and defined in the finite element model as spatial node 39. This location has the largest amplitude for the first mode shape, thus making it the most effective point for the control force.

Having one actuator/sensor pair, the MIMO system, described by equation (12), can be reduced to a SISO system by redefining the following vectors

$$U = F_a; \tag{22}$$

$$B^T = \begin{bmatrix} 0_{M\times 1} & \dfrac{B_c}{M_s} \end{bmatrix} \tag{23}$$

$$C = \begin{bmatrix} 0_{m\times 1} & 0 & 0 & 0_{m\times 1} & 0 & 1 \end{bmatrix} \tag{24}$$

where $\Phi_a = \Phi_{39}$ for the collocated rate feedback control algorithm selected. The root locus of the open-loop transfer function, computed from the SISO state-space variables, described by equations (15), (21), (23), and (24), is plotted in Figure 5. This diagram illustrates the effect of the control gain selection on the complex linear system roots. The desired effect of the control force is to change the roots of the floor system such that they possess a higher degree of damping, i.e., the ratio of the real part of the root to the imaginary part of the root becomes larger while the real portion of the root remains negative. The straight lines labeled with percentages plot this ratio. A root that lies on the line labeled 10% can be said to have approximately 10% damping. A root that possesses a positive real portion has "negative" damping and is, therefore, unstable.

The open-loop poles represent the system roots for the uncontrolled (zero gain) system. The lines connecting the open-loop poles and zeros map possible root locations as the control gain increases from zero to infinity. Individual root locations corresponding to nine specific control gains are plotted. The control gains, ranging from 1.25 to 30, are noted "a" to "i" in Figure 5. These points represent the closed-loop poles (linear system roots for a particular gain value) of the controlled system. Two of the linear system roots are unaffected by the gain selection. These roots correspond to modes 2 and 3 for the floor system, illustrated in Figure 4, which have zero amplitude at the sensor/actuator location. To control these modes, the collocated actuator/sensor must be moved to a floor location where these modes are observable.

The system root labeled A, the proof-mass actuator root, is of particular concern in the controlled system because it is possible to select a gain value for which the real portion of this complex root becomes positive, thus creating unstable behavior in the actuator. This clearly illustrates the fact that, with the inclusion of actuator dynamics, the direct velocity feedback control scheme is no longer unconditionally stable (Balas, 1979). Careful selection of the control gain does, however, produce a stable, robust, and effective control system. The first, fourth and fifth modes of vibration (closed-loop poles) show an increase in damping for each of the selected gain values. The improvement in the dynamic floor properties is reflected in the simulation results presented in the next section.

2.5. Response to Heel-Drop Excitation

The control system can also be evaluated by studying the transient response of the controlled and uncontrolled systems. A heel-drop impact is a convenient excitation to evaluate transient response because it is easy to implement analytically and experimentally. Physically, the standard

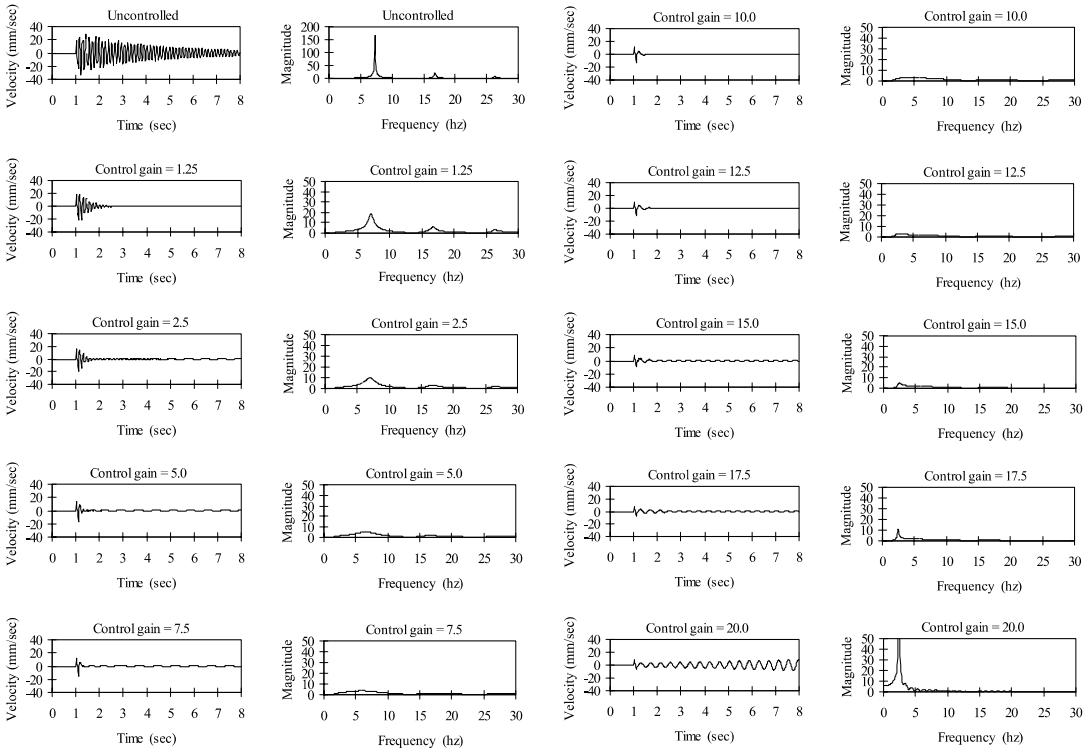

Figure 6. Simulated controlled and uncontrolled floor response.

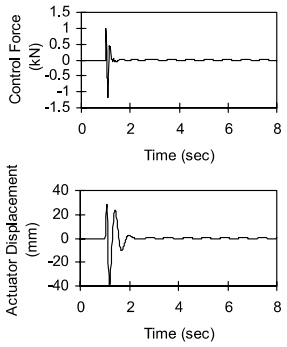

Figure 7. Actuator behavior in linear control system.

heel-drop impact is the force created by an 86.1 kg (190 lb) person standing on their toes and dropping their heels to impact the floor. Analytically, this force is estimated by a 2670 N (600 lb) decreasing ramp function with a 50 ms duration (Murray, 1975). The system response was computed using this decreasing ramp function to excite the floor.

2.5.1. Analytical Study

In the analytical study, the impact, control force (actuator), and velocity measurement were located at the center of the test floor as in the root locus analysis. Ten different cases were computed using various control gains. The time histories and corresponding frequency spectra are plotted in Figure 6. As the control gain is increased, the transient responses of the floor modes are further reduced. This is indicated by a leveling of the sharp peaks noted in the frequency transformation of the velocity time history. The mode around 2 Hz, corresponding to the actuator mass movement, is destabilized by increasing gains. This destabilization begins to have a significant effect on the floor response at gains above 10. The system becomes unstable at a gain of 20 as illustrated previously in the root locus diagram. Control gains between 5 and 10 provide the best performance for controlling the transient response at the center of the floor.

The simulations of the heel-drop response assume the actuator has unlimited stroke length and is unlimited in its ability to produce a control force. Neither case is true. The maximum command input to the amplifier/actuator must be limited to 0.5 V, which produces a maximum control force of 133 N (30 lb). Figure 7 shows the control force and the actuator displacement using the linear controller and excitation studied in the previous section. The control gain selected to illustrate linear control behavior was 7.5. Inspection of the control force graph in Figure 7 reveals that a 1170 N (260 lb) control force is required to achieve the linear control effectiveness illustrated in Figure 6.

Because floor motion increases with increasing disturbance force, a control signal that results from a linear feedback law, such as direct velocity feedback (equation (8)), can become too large and overload the amplifier that drives the proof-mass actuator. The most straightforward approach to prevent overloading the amplifier is to impose a limit on the control signal before it reaches the amplifier. This approach is commonly called a clipping circuit and results in a non-linear control law in the following form

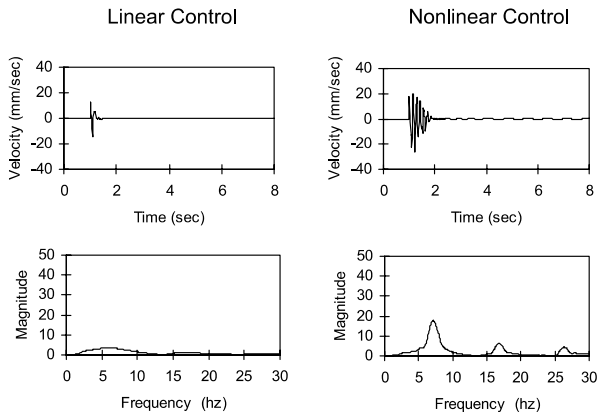

Figure 8. Floor response due to heel-drop excitation for linear and non-linear control.

$$\text{Voltage command} = \begin{cases} v_{\max} & \text{for} \quad \dot{y}_s > \dfrac{v_{\max}}{\text{gain}} \\ \dot{y}_s \cdot \text{gain} & \text{for} \quad \dfrac{v_{\min}}{\text{gain}} < \dot{y}_s < \dfrac{v_{\max}}{\text{gain}} \\ v_{\min} & \text{for} \quad \dot{y}_s < \dfrac{v_{\min}}{\text{gain}} \end{cases} \qquad (25)$$

where $v_{\max}$ and $v_{\min}$ are the limits of the voltage signal to prevent overloading. The graphs in Figure 8 illustrate the effect of this non-linear control law on the control system performance for a heel-drop excitation. The control signal limit results in a control law whose performance is dependent on the magnitude of the excitation and floor response. For small disturbance forces, the controlled system remains linear and can be expected to perform as previously noted. For larger disturbances, the system performance is degraded by the clipping circuit from that predicted by the linear model. Even with the reduced control performance imposed by the actuator limitations, the floor response due to a heel-drop impact is significantly improved over the uncontrolled response.

The floor excitation produced by walking is significantly less than that of a heel drop. Walking excitations will result in the same control effect as noted in the linear control studies, because they produce maximum control forces in the linear region of the control law. The control signal limit will be shown in the following section to have little effect on the control performance for walking-induced vibrations of the actual floor system.

2.5.2. Experimental Verification

There are two objectives behind the following evaluation of control effectiveness for heel-drop excitations. The first objective is to confirm the theoretical system model derived and implemented in the simulation study. The second is to compare and evaluate the experimental results for the uncontrolled and controlled systems when subjected to a transient excitation such as the heel-drop impact.

The control actuator and sensor were, as in the simulation studies, placed at the center of the test floor where the largest vibration amplitudes exist. Because the response of the floor system is dependent on the excitation, a reasonable comparison of the simulated and experimental floor responses is most accurately obtained by using the experimentally measured excitation as the input to the simulation model. Otherwise, discrepancies between the simulated and experimental response may be due to differences in the excitation rather than inaccuracies in the analytical floor model. A force plate, constructed of four load cells supporting a 406 mm square steel plate, was used to measure the actual excitation force produced by a person performing a heel-drop impact.

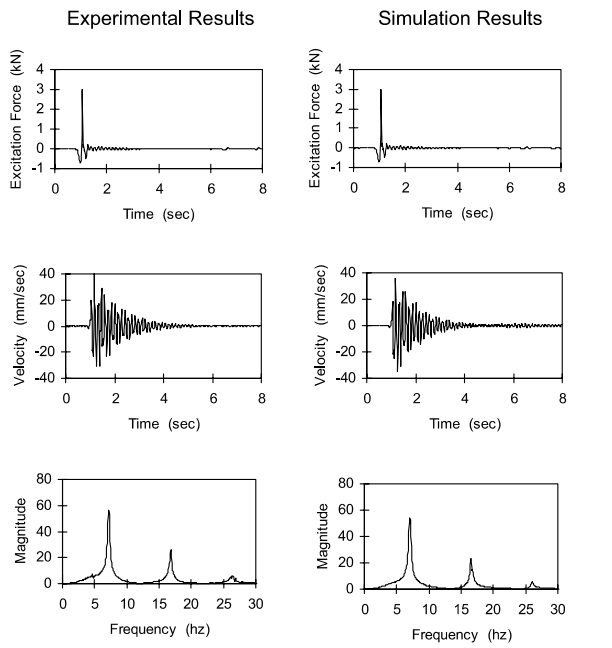

Figure 9. Uncontrolled experimental and simulated response due to a heel-drop excitation.

A heel-drop excitation is useful in evaluating the transient behavior of the system. Both the excitation force and the velocity response were recorded with the controller off. The response was then simulated using the measured excitation as force input. Figure 9 compares the simulation and experimental data at the center of the test floor with the controller off. This figure illustrates that the uncontrolled system response is accurately predicted by the analytical model for that location on the test floor.

Similar experiments and simulations were conducted for the controlled system. With the actuator and sensor at the center of the floor, the feedback gain was programmed and tested between 2.5 and 17.5 in increments of 2.5. The voltage command to the actuator was limited to ± 0.5 V so as not to exceed the force limitation of the actuator. A heel-drop impact was performed by a person standing on the force plate next to the actuator for each gain value noted above. Measurements were simultaneously recorded from the force plate and the velocity sensor. The gain producing the most significant reduction in the transient vibration levels was 7.5. This matches the results found in the simulation study as illustrated in Figure 6.

Using the experimentally measured force from the heel-drop test (7.5 gain controller) as an input excitation, a simulation of the response was computed. The results from this experiment and simulation are presented in Figure 10. Inspection of the results reveals a very accurate prediction

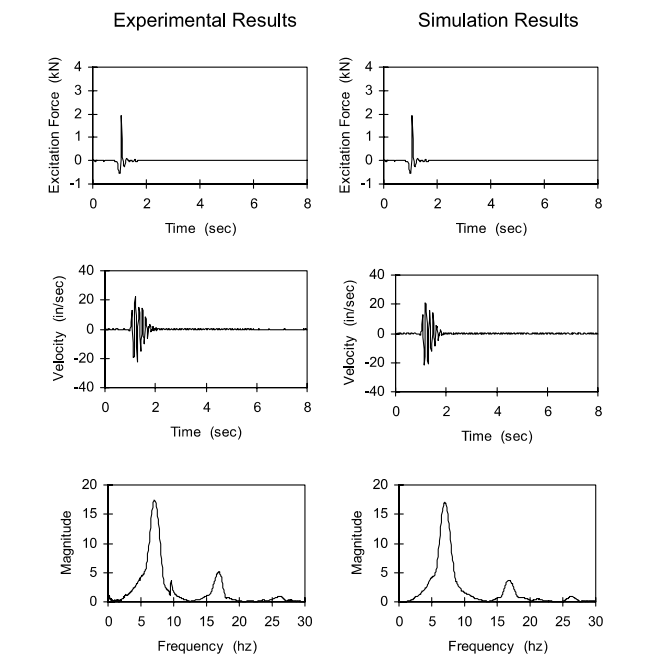

Figure 10. Controlled experimental and simulated response due to a heel-drop excitation.

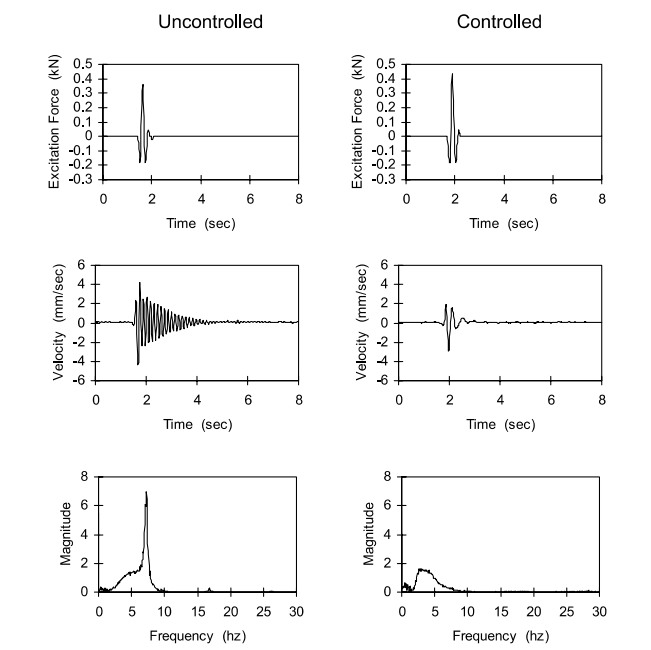

Figure 11. Uncontrolled and controlled experimental response due to a small impact-like excitation.

of the controlled system using the analytical model developed. The results presented in this figure are very dependent on the non-linear capabilities of the controller as was theoretically illustrated previously.

The results already presented can be re-evaluated to reflect control system effectiveness rather than analytical model accuracy. The concept of equivalent viscous damping (Tedesco et al., 1999) is useful in assessing the non-linear control effectiveness. Equivalent viscous damping provides a means to approximate the energy dissipation characteristics of a non-viscous system. The method of quadrature peak picking (Inman, 1994, p. 379) can be used to compute the equivalent viscous damping for a specific excitation level. The uncontrolled system of Figure 9 has 2.2% equivalent viscous damping in the first floor mode, while the controlled response of Figure 10 represents 9.7% equivalent damping.

It should be noted that the linear control system studied in the simulations possessed approximately 40% damping in the first floor mode, much greater than the 9.7% calculated from Figure 10. The 40% damping level in the simulations was determined from the calculation of the linear system roots for the controlled system. To experimentally achieve the same level of damping as the linear system, the floor must be excited within the linear range of the controller. To achieve this, the experiments performed for the heel-drop excitation were repeated using a smaller impact-like excitation. This smaller excitation was accomplished by having the person standing on the plate flex their knees and then stand straight again. Results from this experiment are shown in Figure 11.

The method of quadrature peak picking is only effective for predicting the equivalent viscous damping in well-spaced, lightly-damped (<20%) modes. The evaluation of the control system effectiveness for the small impact-like excitation is therefore more qualitative than quantitative. A comparison of the graphs in Figure 11 reveals a nearly complete removal of the transient component in the floor response for the controlled system. This behavior reflects the effectiveness illustrated for the linear controller simulation studies, that is, an equivalent viscous damping of approximately 40% for the first floor mode as described previously.

2.6. Response to Walking Excitation

The objective of studying the control system for walking excitations was to compare experimental results for the uncontrolled and controlled system responses. In this set of experiments, the actuator and velocity sensor were located at the center of the floor. The excitation was due to a person walking parallel to the joists close to the center of the 15 ft span. During the 16 s time measurement, the person traversed the length of the floor two times. The largest amplitudes were measured when the pedestrian was near the center of the floor and the small amplitudes were measured as the walker turned around near each girder. In the controlled system responses, the voltage command to the shaker was again limited to ±0.5 V. As in the heel-drop experiments, the feedback gain was programmed between 2.5 and 17.5 in increments of 2.5. A feedback gain of 7.5 produced the most significant reduction in floor vibration amplitudes. The experimental time measurements of the uncontrolled and controlled (gain = 7.5) system response, due to walking excitations, are presented in Figure 12. The peak amplitude in this controlled response is approximately 12% of the peak amplitude for the uncontrolled system as shown in Figure 12.

2.7. Stability Properties

Perhaps the primary concern in the implementation of active structural control is the system stability. The concept of stability was addressed in the analytical discussion of

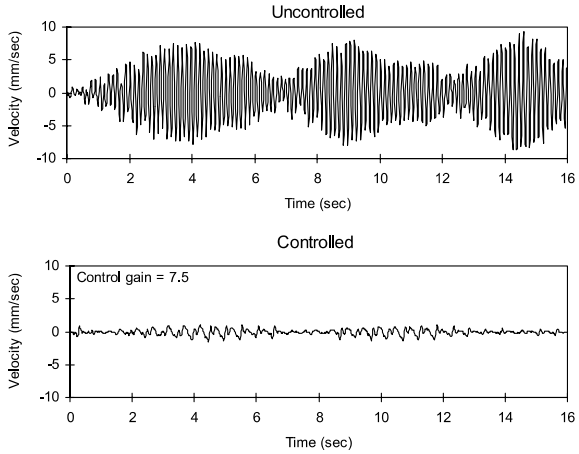

Figure 12. Uncontrolled and controlled experimental response to walking excitations.

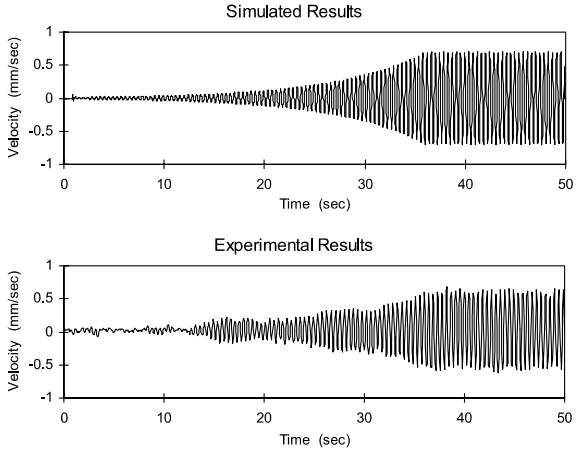

Figure 13. Simulated and experimental floor response for an unstable control gain.

the linear system roots and the root locus. As noted in this discussion, actuator dynamics can produce instabilities in the system if the control gain is not carefully selected. The purpose here is not to reiterate the discussion, but rather to experimentally verify the analytical behavior with respect to stability.

For the analytical model, the stable gain range was 0 to 19.53. The performance of the controller was shown to be affected by the degree of stability maintained in the actuator root, labeled "A" in Figure 5. The most effective gain selection for controlling the system was not the largest possible stable gain. Instead, a gain which controlled the floor response while maintaining a moderate degree of stability in the actuator root provided the best control performance. This behavior was experimentally verified as presented in Figure 10 where 7.5 was the control gain. Although data were not presented, gains up to 17.5 were tested and found to be stable.

Theoretically, unstable behavior is predicted for gains above 19.53. To verify this prediction, a gain selection of 20.0 was implemented experimentally. The initial disturbance in the system was the result of electrical noise in the system. The velocity time history of the floor response (at the center of the test floor) from this experimental test is shown, along with the simulated response, in Figure 13. In the simulation, a small impact excitation was used as the initial disturbance. Within the linear range of the controller, the magnitude of the floor response increased exponentially as would be expected in the unstable system. The response then leveled off to a steady-state oscillation. This is the result of the command limiter built into the control algorithm. A destructive unstable behavior, with amplitudes increasing to failure, is not possible with the non-linear control parameters in equation (25) properly selected. In fact, the steady-state oscillation produced by a linearly unstable gain selection, above 19.5 for the experimental system, is found to produce only a slightly perceptible vibration level.

By selecting the most effective control gain for controlling walking vibrations, a comfortable margin of stability in the linear system is maintained. Additionally, the non-linear circuit provides a safeguard against destructive behavior from an unstable gain selection.

2.8. Comparison of Active and Passive Control

The most closely related traditional repair measure to the active device is the tuned mass damper (TMD). An analytical study was undertaken to compare the active and passive systems with respect to controlling floor vibrations. In this study, analytical simulations of the floor response are computed to illustrate the benefits of active control over a passive device. Two TMD designs were used with the analytical model of the experimental floor to compare their relative effectiveness with that of the active control implementation. The excitation studied in the comparison is a theoretical heel drop. The control actuator or TMD, the excitation force, and the floor response are at the center of floor, node 39 in the finite element model.

The *Shock and Vibration Handbook* (Reed, 1988) provides equations for designing and optimizing the parameters of a tuned mass damper as follows:

$$\omega_n = \sqrt{\frac{K_1}{M_1}}; \tag{26}$$

$$\mu = \frac{M_2}{M_1}; \tag{27}$$

$$\omega_{opt} = \omega_n \frac{1}{1+\mu} = \frac{K_2}{M_2}; \tag{28}$$

$$\zeta_{opt} = \sqrt{\frac{\mu}{2(1+\mu)}} = \frac{C_2}{\sqrt{K_2 M_2}}. \tag{29}$$

Here, M_1, C_1, and K_1 are the single-degree-of-freedom (SDOF) floor system parameters for mass, damping, and stiffness, respectively, computed from the first mode properties of the floor model, and M_2, C_2, and K_2 are the optimized TMD parameters for mass, damping and stiffness, respectively.

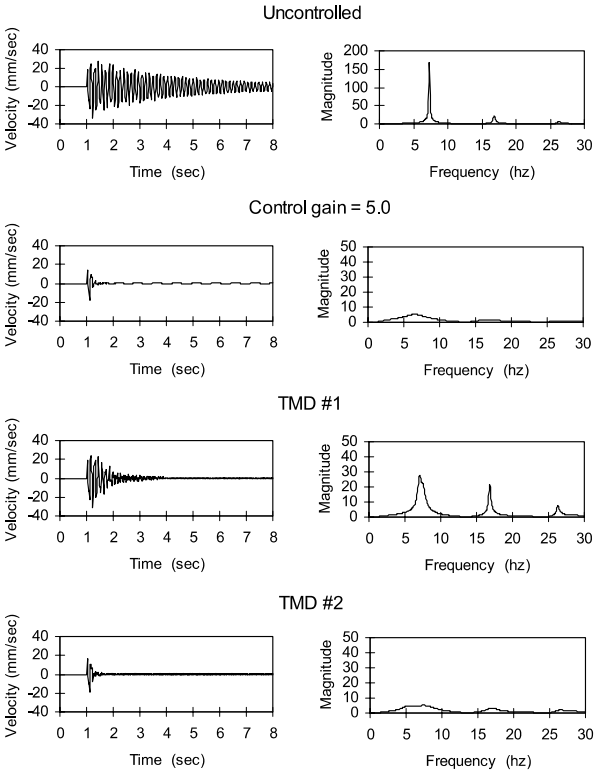

Figure 14. Analytical comparison of TMD and active control effectiveness.

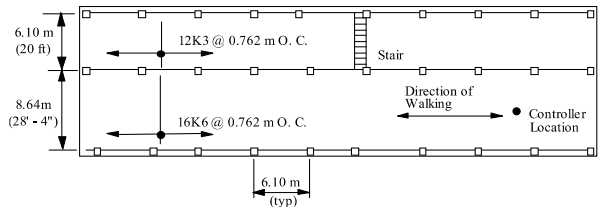

Figure 15. Office floor plan.

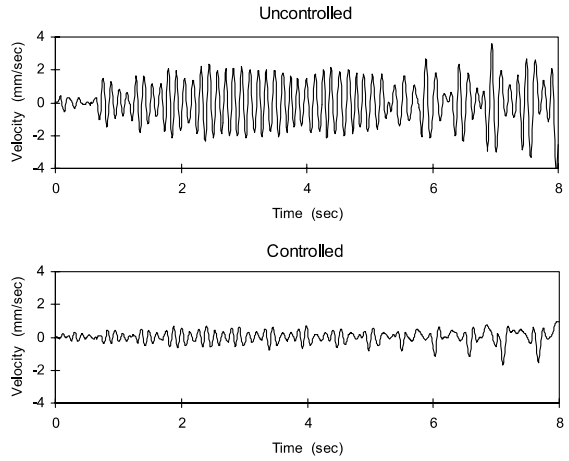

Figure 16. Uncontrolled and actively controlled response of an office floor.

Table 3. Floor system and TMD properties.

	Floor System		TMD1		TMD2
M_1	2973 kg (6554 lb)	M_2	30.4 kg (67 lb)	M_2	907 kg (2000 lb)
C_1	1.296 kN (m s^{-1})$^{-1}$	C_2	0.1975 kN (m s^{-1})$^{-1}$	C_2	22.08 kN (m s^{-1})$^{-1}$
K_1	6394 kN m^{-1}	K_2	63.90 kN m^{-1}	K_2	1147 kN m^{-1}

Using this procedure, two TMDs were designed for implementation in the analytical model. One damper was designed to illustrate the TMD control effectiveness using a passive reaction mass, 30 kg (67 lb), equivalent to the moving mass in the active control device. The second TMD was designed to provide 20% equivalent damping in the first mode of vibration of the floor system. This performance is achieved in the active system with a control gain of 5. Table 3 shows the properties for the floor system and the two TMDs described above.

The floor response due to a heel-drop impact was computed for the uncontrolled system, the actively controlled system, the TMD1 controlled system, and the TMD2 controlled system. The excitation, control force (active or TMD), and the measurement were located at the center of the floor. The time histories and corresponding frequency spectra are plotted in Figure 14.

Results from the analytical study show that a tuned mass damper possessing an equivalent reactive mass, TMD1, increases the damping in the first mode from 0.5% to 3.8% as compared to the 20% damping supplied by the active damper. The TMD designed to provide 20% damping in the first mode of vibration, TMD2, is very effective but has 30 times the weight of the active mass. This is more than 30% of the primary mass, M_1, of the mode being controlled. This amount of weight would be impractical for installation on a floor. Because the active damper is smaller and lighter, it could easily be installed in the ceiling cavity below most problem floors. This study clearly illustrates the performance benefits of active over passive control in this application.

2.9. Results from Temporary Installations

Case studies describing two temporary installations are presented to illustrate the effectiveness of the active control scheme on two occupied floors.

2.9.1. Improving a Problem Office Floor

An office floor in a light manufacturing facility was reported to have annoying levels of occupant-induced floor vibrations. A plan of this floor is shown in Figure 15. The construction of this floor consists of a 63 mm (2.5 in) lightweight concrete slab on a metal deck supported by joist framing members as indicated on the plan. The 8.64 m (28

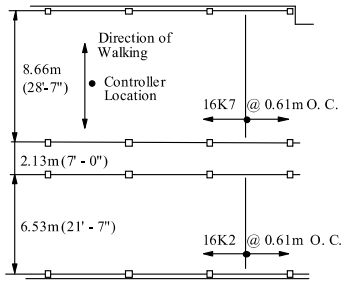

Figure 17. Chemistry laboratory floor plan.

ft 4 in) span was found to be the problem area. In this span, two long rows of desks are separated by an aisle near the center of the span. This open office area is used primarily for order processing with personal computers on nearly every desk. Walking in the aisle causes computer monitors to rock, thus intensifying the degree of annoyance. One particularly disturbing characteristic of this floor is that annoying levels of vibration are felt even when the occupant movement is several bays away.

An attempt was made to actively control the floor movement at a location where the problem was particularly acute. The control actuator and sensor were placed at the controller location noted in Figure 15. The floor response due to a person walking in the aisle between the desks was measured for the uncontrolled and controlled system. To provide a valid comparison, care was taken to keep the walking excitation as consistent as possible for the two measurements. A comparison of the results for the uncontrolled and controlled system is shown in Figure 16. For each vibration measurement the root-mean-square (rms) acceleration was calculated. The uncontrolled floor system had an 8 s rms acceleration level of 0.0057g while the controlled system had a level of 0.0017g. This represents more than a 70% reduction in the vibration level.

2.9.2. Improving a Problem Chemistry Laboratory Floor

Excessive floor vibration due to occupant movement was reported to exist in a chemistry laboratory where sensitive microscopes were in use. A partial plan of the floor system is shown in Figure 17. The 2.13 m (7 ft) span is a corridor with laboratory rooms on either side. The floor construction consists of a 90 mm (3.5 in) concrete slab on metal deck supported by joist members as shown in the plan. The problem area, in the laboratory with the 8.71 m (28 ft 7 in) span, contains three island-type workbenches where the function has been impaired due to disturbing levels of floor vibration.

The active control scheme was implemented to reduce the floor motion. Several tests were performed to assess the effectiveness of the control. Results from the walking excitation tests are shown in Figure 18. For this test, the control actuator and sensor were placed between two of the workbenches. This location is noted in Figure 17. From the data shown in the graphs, the uncontrolled rms acceleration was computed to be 0.0037g for the 8 s uncontrolled response and 0.0009g for the 8 s controlled response. This represents over a 75% reduction in the vibration level.

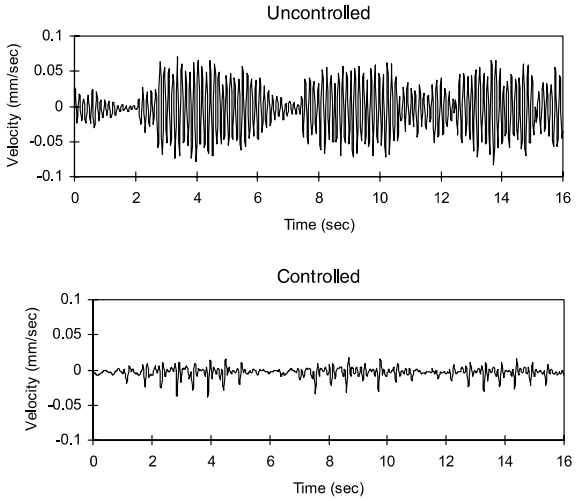

Figure 18. Uncontrolled and actively controlled response of a chemistry laboratory floor.

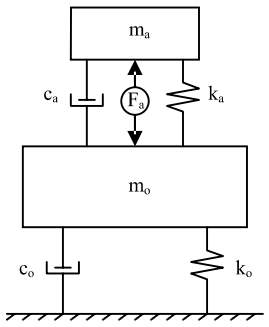

Figure 19. SIMO system model.

3. Single-Input/Multi-Output Control Research

Research implementing a single-input/multi-output (SIMO) control design is described in this section. The main goal of this research is to improve the ability of a single actuator to suppress objectionable vibrations. The effectiveness of the SIMO controller developed is illustrated through simulation studies using a simplified analytical model.

3.1. State-Space Model

A state-space model is developed in this section to study the effect of adding additional output feedback variables to the SISO control scheme discussed previously. The floor system is modeled as a SDOF system representing the maximum participation of the fundamental mode response. The maximum participation of the fundamental mode is physically located at the center of the experimental test floor. Such a model is justified because the fundamental mode response is usually the primary contributor to human discomfort in problem floors (Murray et al., 1997). The control actuator, illustrated in Figure 3, adds a second degree of freedom to the controlled system model shown in Figure 19. The equations of motion for this system are as follows:

Table 4. Floor system variables for SIMO study.

Floor Parameter	Floor 1: 7.4 Hz	Floor 2: 2.0 Hz
m_0	2973 kg (6554 lb)	2973 kg (6554 lb)
c_0	1.296 kN (m s^{-1})$^{-1}$	0.3730 kN (m s^{-1})$^{-1}$
k_0	6394 kN m^{-1}	466.9 kN m^{-1}

$$\begin{bmatrix} m_0 & 0 \\ 0 & m_a \end{bmatrix}\begin{Bmatrix} \ddot{y}_0 \\ \ddot{y}_a \end{Bmatrix}+\begin{bmatrix} c_0+c_a & -c_a \\ -c_a & c_a \end{bmatrix}\begin{Bmatrix} \dot{y}_0 \\ \dot{y}_a \end{Bmatrix}$$

$$+\begin{bmatrix} k_0+k_a & -k_a \\ -k_a & k_a \end{bmatrix}\begin{Bmatrix} y_0 \\ y_a \end{Bmatrix}=\begin{Bmatrix} F_d-F_a \\ F_a \end{Bmatrix}. \quad (30)$$

Here, $\ddot{y}_0$, $\dot{y}_0$, and y_0 are the floor acceleration, velocity, and displacement, respectively; F_d is the disturbance force on the floor; F_a is the actuator force acting between the actuator and floor mass; m_a, c_a, and k_a, specified in Table 1, are the actuator properties; m_0, c_0, *and* k_0 are the simplified floor properties defined for two floor systems in Table 4.

The equations represented in equation (30) can be expressed in the state space by defining the state-space variables in the general form

$$\dot{\mathrm{X}}=\mathrm{AX}+\mathrm{BU}$$

$$\mathrm{Y}=\mathrm{CX}+\mathrm{DU} \quad (31)$$

where $\mathrm{X}^{\mathrm{T}}=\{x_1\ x_2\ x_3\ x_4\}=\{y_0\ \ y_a\ \ \dot{y}_0\ \ \dot{y}_a\}$ is the state variable vector, Y^{T} is the output vector, and

$$\mathrm{A}=\begin{bmatrix} 0 & 0 & 1 & 0 \\ 0 & 0 & 0 & 1 \\ -\dfrac{k_0+k_a}{m_0} & \dfrac{k_a}{m_0} & -\dfrac{c_0+c_a}{m_0} & \dfrac{c_a}{m_0} \\ \dfrac{k_a}{m_0} & -\dfrac{k_a}{m_0} & \dfrac{c_a}{m_0} & -\dfrac{c_a}{m_0} \end{bmatrix} \quad (32)$$

$$\mathrm{U}=\begin{Bmatrix} F_d \\ F_a \end{Bmatrix} \quad (33)$$

$$\mathrm{B}^{\mathrm{T}}=\begin{bmatrix} 0 & 0 & 1/m_0 & 0 \\ 0 & 0 & -1/m_0 & 1/m_a \end{bmatrix} \quad (34)$$

$$\mathrm{C}=\begin{bmatrix} -1 & 1 & 0 & 0 \\ 0 & 0 & 1 & 0 \\ 0 & 0 & 0 & 1 \end{bmatrix} \quad (35)$$

$$\mathrm{D}=[0\ \ 0]. \quad (36)$$

The output matrix, C, can take any form depending on which output values are available and selected for the feedback control algorithm. The above form indicates three experimentally measurable outputs, namely, actuator mass displacement relative to that of the floor mid-span point, mid-span floor velocity, and actuator mass velocity.

A control force, F_a, is generated according to the following control law

$$F_a=G_1y_1+G_2y_2\ldots \quad (37)$$

or in matrix form

$$F_a=\begin{bmatrix} G_1 & G_2 & \cdots \end{bmatrix}\begin{Bmatrix} y_1 \\ y_2 \\ \vdots \end{Bmatrix}=GY \quad (38)$$

where F_a is the control force introduced to suppress the disturbance induced vibration, Y is the measured output vector, and G is a row matrix containing the feedback gain values.

3.2. Multi-Output Feedback Control Design

Output feedback gains are selected to satisfy several performance and stability conditions. For heel-drop excitation, the gains are selected to give a short settling time thus minimizing the effect of the annoying transient response. For walking excitation, it is desired to suppress the amplitudes of a steady-state floor motion. In the SISO case, it was reasonable to use a trial-and-error process to select the best control gain. This approach becomes impractical for the SIMO controller. To design the SIMO controller, the concept of a performance index (PI) is implemented. An appropriately configured PI provides a quantitative measure of the performance for different sets of G (Ogata, 1990, p. 68) that, when minimized, provides the most effective controller.

To understand the derivation of the frequency domain based PI developed herein, a brief overview of a commonly used floor vibration criterion is presented. Murray et al. (1997) recommend the following criterion for assessing proposed floor system designs that will be subjected to walking excitation

$$\frac{a_p}{g}=\frac{P_0\ \exp(-0.35f_n)}{\beta W}\le\frac{a_0}{g} \quad (39)$$

where a_p/g is the estimated peak acceleration, a_0/g is the acceleration limit found acceptable with respect to human perception for a given occupancy, f_n is the first natural frequency of the floor structure, P_0 is a force constant, β is the damping ratio of the fundamental floor mode, and W is the effective weight of the fundamental floor mode. The basis for this criterion is that walking excitation produces a sinusoidal input force that is in resonance with the first natural frequency of the floor system. The sinusoidal input force is frequency-dependent with a peak amplitude equal to $P_0\ \exp(-0.35f_n)$ where P_0 is 0.29 kN (65 lb) for most floor systems.

The system equations (equations (31)–(36)) are used to determine the steady-state acceleration amplitudes of the floor system throughout a certain frequency span for a given set of control gains as follows

$$\ddot{Y}_0(f_n)=\left|\frac{\dot{Y}_0}{F_d}\right|(2\pi f_n)65\exp(-0.35f_n) \quad (40)$$

where $\left|\dot{Y}_0/F_d\right|$ is the magnitude of the frequency response function of the velocity output of the floor mass and a dis-

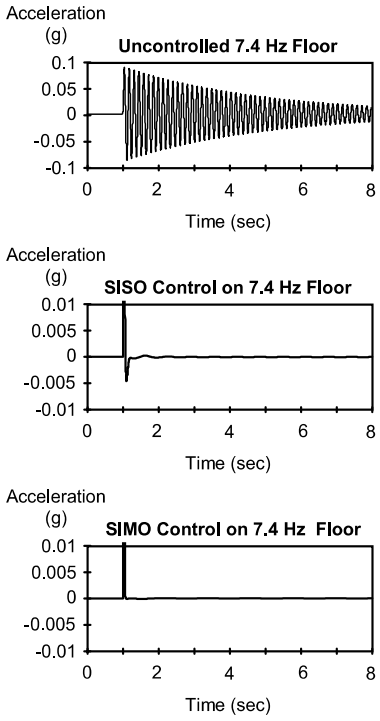

Figure 20. Comparison of active control effectiveness for 7.4 Hz floor.

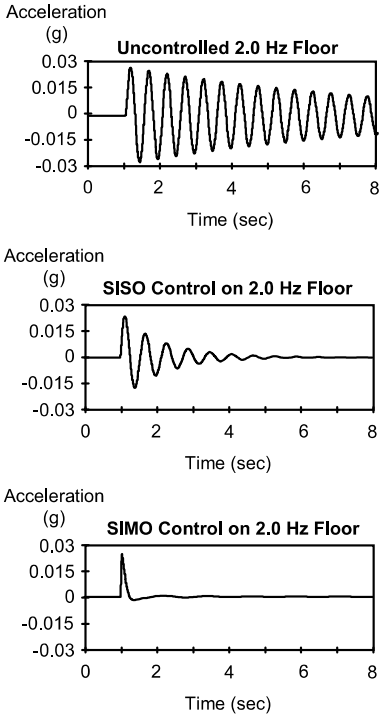

Figure 21. Comparison of active control effectiveness for 2.0 Hz floor.

Table 5. Comparison of results for SIMO controller designs.

Floor Frequency	Controller Design	Relative Displacement Feedback Gain	Floor Velocity Feedback Gain	Actuator Velocity Feedback Gain	Steady-State Acceleration Amplitude
7.4 Hz	Uncontrolled	0	0	0	0.0670 g
	SISO	0	1270	0	0.00070 g
	SIMO	11.5	4120	0.142	0.00027g
2.0 Hz	Uncontrolled	0	0	0	0.224 g
	SISO	0	72	0	0.0321 g
	SIMO	11.5	220	0.28	0.0044 g

Note: Steady-state acceleration amplitudes above 0.005 g would be considered unacceptable in an office occupancy (Murray et al., 1997).

turbance input to the floor. The performance index, J, for a particular set of stable control gains denoted as case i, is the maximum value of the function $\ddot{Y}_0(f_n)$:

$$J(i) = \max(\ddot{Y}_0(f_n, i)) \text{ for the } i\text{th set of control gains.} \quad (41)$$

The stability of a particular set of control gains is determined by the controlled system roots as described in Section 2.4. This performance index can be evaluated for an array of stable control gains, whereby the minimum J would identify the most effective set of control gains for minimizing the steady-state floor acceleration.

3.3. Analytical Results

Two different floor systems were studied to illustrate the effectiveness of expanding the SISO controller to a SIMO controller. The properties of these floor systems are presented in Table 4. Although the following results were obtained using the frequency domain PI described previously, similar results can be obtained using the other suggested PIs.

The last column of Table 5 shows the maximum steady-state acceleration amplitude due to a simulated walking excitation for six cases. Focusing on the 7.4 Hz floor, we should note that a dramatic reduction in the acceleration amplitude is achieved by the SISO controller. Although further reduction is noted for the SIMO controller, the change from the SISO to SIMO is not significant. We can conclude that the additional hardware is not justified by such a marginal improvement. This is not the case for the 2.0 Hz floor. The SISO controller reduces the uncontrolled amplitude by a factor of 7. The additional feedback vari-

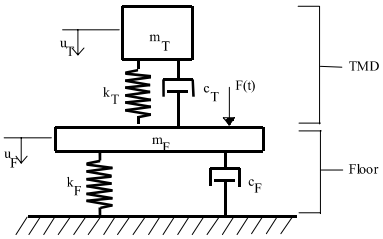

Figure 22. Two-degree-of-freedom model of TMD and floor.

ables provide a further reduction by another factor of 7. In more concrete terms, the SISO controller does not reduce the acceleration amplitude below the acceptable limit (0.005 g) for an office occupancy. The SIMO controller does.

The effectiveness of the controller is also illustrated in Figures 20 and 21. Each of the six floor systems was subjected to a simulated heel-drop impact. On the 7.4 Hz floor, the most dramatic change in the transient response is noted between the uncontrolled case and the SISO controlled case. On the 2.0 Hz floor, the transient response dissipates much more quickly for the SIMO controlled case.

4. Passive Control Research Using TMDs

Passive control, as it is applied in this research, refers to a device or devices that do not need an external energy source to alter the dynamic behavior of a structural system. The passive control mechanism implemented is a TMD, which, when properly tuned, reduces both resonant and transient vibration levels. A common TMD consists of a spring in parallel with a damping element connecting the floor mass with the TMD mass. Figure 22 illustrates a two-degree-of-freedom system that represents a simplified model of the floor system with a TMD. The floor is modeled by a SDOF system because a TMD, by its inherent properties, only targets one mode of vibration for control. However, in the case of building floor vibrations, more than one mode is usually excited by human activity. Therefore, to eliminate all annoying vibrations, it may be necessary to install more than one TMD in a bay.

To achieve the highest level of vibration control for a given TMD mass, the stiffness and damping elements must be optimized based on the properties of the floor system being controlled. Equations for the optimized parameters were presented for purposes of comparison in Section 2.8 of this paper. In an optimized TMD, the stiffness and mass elements of the TMD must be adjusted such that the natural frequency of the TMD is slightly less than the frequency of the floor system. The magnitude of each parameter is roughly determined in the design of the TMD. In the final application, the mass is then varied to fine tune the TMD. For maximum effectiveness, the TMD should be placed at a point of maximum amplitude for the mode of vibration it is to control.

4.1. Tuned Mass Dampers

Two different TMDs were used in this research. The first consists of a steel plate as the spring, and two stacks of steel plates, acting as additional mass, that were used to adjust the TMD frequency (Shope and Murray, 1995). Damping is provided by liquid filled bladders confined in two rigid containers instead of conventional dashpot or damping elements connecting the additional mass to the original structure. A schematic diagram of the TMD is shown in Figure 23. This TMD type will be referred as the liquid-TMD.

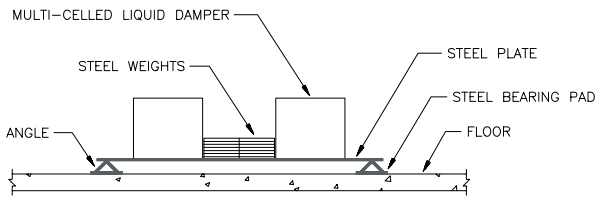

Figure 23. Liquid-TMD.

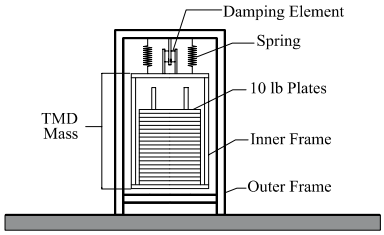

Figure 24. Visco-TMD.

The second type of TMD used in this research is shown in Figure 24 (Hanagan et al., 1996; Rottmann and Murray, 1997). These dampers were designed by the 3M Company, St Paul, Minnesota, and consist of an outer frame that rests on the floor, connecting elements, and an inner frame. Four springs and a visco-elastic damping element connect the outer frame to the inner, mass carrying frame. The inner frame can hold a number of steel plates, which provide the mass for the TMD and allow for tuning. Three dampers of this type were used in the research and will be referred to as the visco-TMDs.

4.2. Results from Laboratory Tests

The liquid-TMDs were tested on the laboratory floor that was described previously (Shope and Murray, 1995). The free vibration response of the floor was measured by conducting an impact test commonly known as a heel-drop test (Murray, 1975). The standard heel-drop test is performed by first standing on the balls of the feet, then leaning back allowing the heels to impact the floor. The response of the floor is measured and a fast Fourier transform (FFT) is then performed on the acceleration history to extract the response spectrum of the system. The resulting data indicate that the floor has two strong modes of vibration, one at 7.3 Hz and the other at 17 Hz.

To control the floor, four liquid dampers were used, two for each mode. The dampers were tuned by first placing them on a rigid surface and adjusting the mass so that the frequency was approximately 0.5 Hz below the modal frequency. Changing the mass, the plate span, or both per-

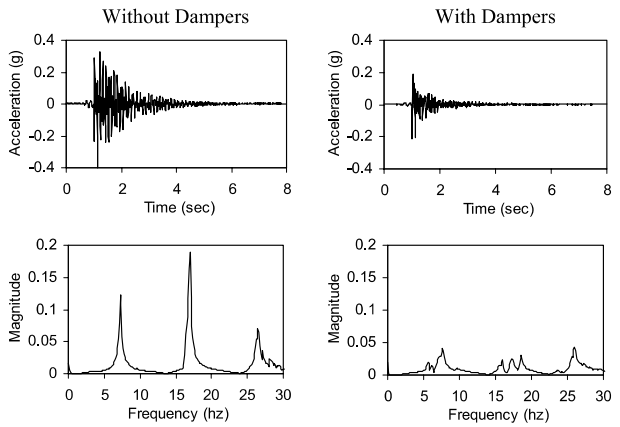

Figure 25. Heel-drop induced response of a laboratory floor without and with liquid-TMDs.

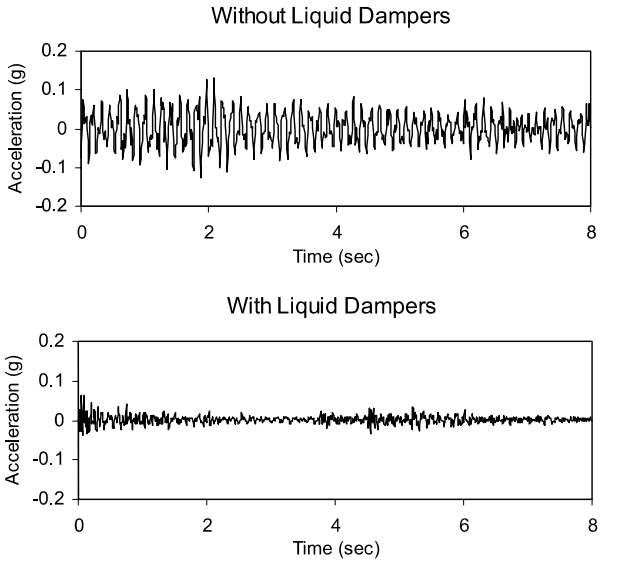

Figure 26. Walking induced response of the laboratory floor without and with liquid-TMDs.

forms tuning. Once tuned, the dampers were positioned on the floor such that one end was located over the point of maximum amplitude for the mode shape under consideration. It was also important that there were no nodes of the mode shape located between the two ends of the damper. Otherwise, the damper would tend to rotate as a rigid body and would not achieve the desired result. Once in place, final adjustments were made to the mass to optimize performance.

Figure 25 shows the heel-drop acceleration time histories and corresponding frequency spectra for the laboratory floor with and without the dampers. The figure illustrates that there was very little damping inherent in the original floor. Without the dampers, the vibration took more than 3 s to decay. Conversely, the vibration of the floor with dampers took only 1 s to decay. The small amount of damping in the original floor is also illustrated by the two sharp peaks in the uncontrolled frequency spectrum at 7.3 and 17 Hz. The spectrum for the controlled condition shows that these peaks are nearly eliminated by the dampers.

Figure 26 shows the acceleration histories of the floor with and without dampers while a person walked along the mid-span. The average peak accelerations were reduced from 0.06 g to 0.01 g after the dampers were installed. Not only was a significant reduction in peak accelerations observed, but also the damped acceleration response consisted mainly of high-frequency vibration that is generally found to be less annoying to occupants.

The visco-TMDs were also tested on the laboratory floor (Rottmann and Murray, 1996). Additional heel-drop testing showed that the floor lowest modes were at 7.375, 9.375, and 16.75 Hz. The mode shapes associated with these measured modes are shown in Figure 27. Visco-TMDs were placed at locations of peak displacement for the mode of vibration for which they were designed to control: one at the center of the floor to control the first mode, the second at an edge to control the second mode, and the third at the opposite edge to control the third mode. The second and third mode peak displacements are both at the center of the span at the free edges. Visco-TMD1, which was designed to control the fundamental mode, was placed first on the floor and tuned by adding or removing steel plates. "Optimum" performance was obtained when the TMD had a frequency of 6.45 Hz and a TMD mass-to-floor mass ratio of 0.057. With visco-TMD1 on the floor, visco-TMD2 was placed on the floor to control the third mode of vibration. "Optimal" control of mode 3 was achieved when visco-TMD3 had a frequency of 15.94 Hz and a TMD mass-to-floor mass ratio of 0.0912. Visco-TMD2 was finally placed on the floor and "optimally" tuned to a frequency of 9.17 Hz with a mass ratio of 0.0570. Once all three visco-TMDs were in place, the mass of visco-TMD1 was increased further improving the floor vibration control. This TMD, visco-TMD1a, had a frequency of 5.84 Hz.

Figure 28 shows the accelerations at the center of the laboratory floor due to a heel-drop impact at the center of the floor and the corresponding FFT, with and without the TMDs in place. Figure 29 shows accelerations at the center of the bay due to a person walking parallel to the joists and due to a person walking perpendicular to the joists with and without the TMDs in place. The rms of the data over the total time interval of the measurement was determined and was used to compare the change in overall acceleration from one floor condition to another. The rms acceleration due to walking parallel to the joists was reduced by a factor of 5.5 and by a factor of 3.7 for walking perpendicular to the joists.

4.3. Results from Field Tests and Installations

Case studies describing two permanent installations are presented to illustrate the effectiveness of the passive control scheme on occupied floors.

4.3.1. Building 1

Because of complaints indicating annoying floor motion on the second floor of a new office building, liquid-TMDs were installed in three bays of the building (Shope and Murray, 1995). A plan is shown in Figure 30. The floor

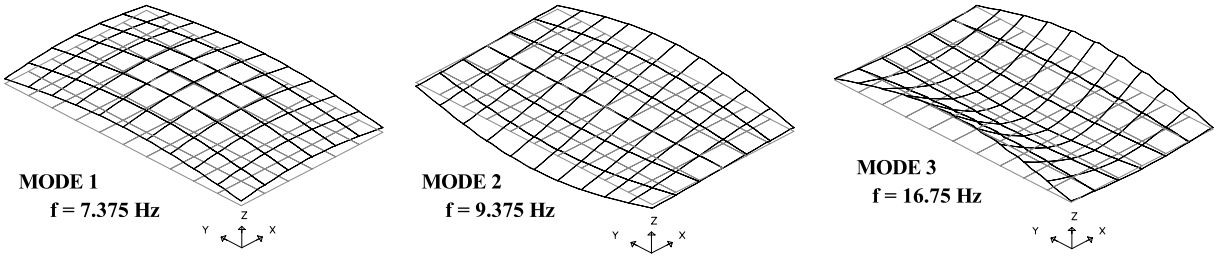

Figure 27. Mode shapes for laboratory floor.

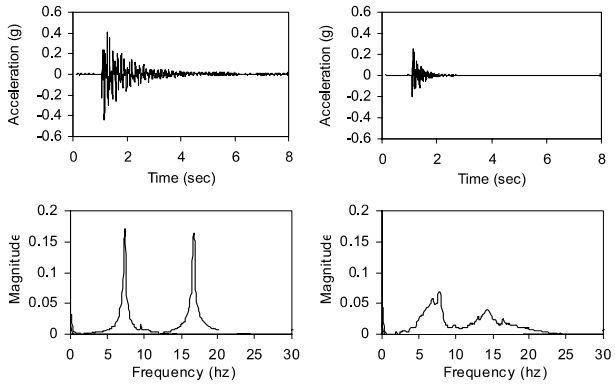

Figure 28. Heel-drop induced response of a laboratory floor without and with visco-TMDs.

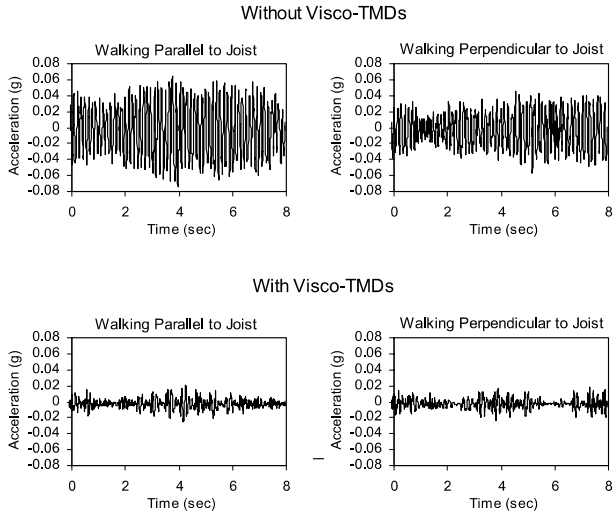

Figure 29. Walking induced response of the laboratory floor without and with visco-TMDs.

system consists of 114 mm (4.5 in) total depth normal weight concrete on a 51 mm (2 in) metal deck, open web joists and joist girders. The joists are spaced at 1.22 m (48 in) on-center and span 15.85 m (52 ft); the joist girders span 4.88 m (16 ft). Heel-drop impact tests identified a significant dynamic response at two natural frequencies, 5.1 and 6.5 Hz.

To decrease the magnitude of the floor motion, 14 liquid-TMDs were installed. The dampers were hung from the

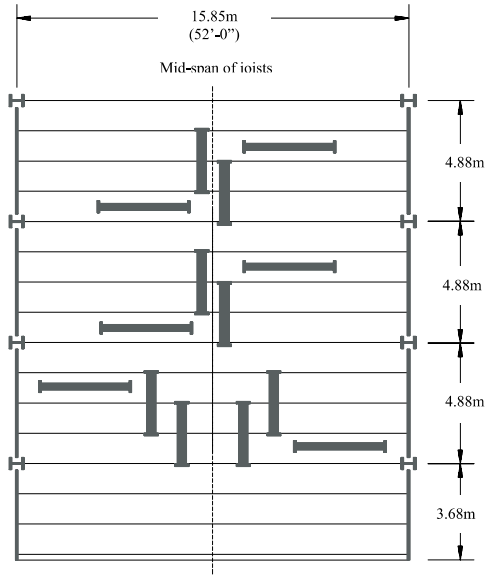

Figure 30. Placement of liquid-TMDs on office floor of building 1.

bottom chords of the existing floor joists and were located as shown in Figure 30. The dampers oriented perpendicular to the joists were used to control the first mode of vibration (5.1 Hz) and those oriented parallel to the joists were used to control the second mode (6.5 Hz). The dampers were first tuned while mounted on a rigid support. After they were attached to the joists, a second tuning was carried out to improve the performance of the floor.

Figure 31 shows acceleration histories for a person walking perpendicular to the joist span before and after the installation of the dampers. A significant improvement in the floor response is evident. The response from occupants using the improved floor was reported to be "very positive".

4.3.2. Building 2

Complaints of annoying floor vibrations on the second floor of an office building led to testing of the visco-TMDs on the office floor (Rottmann and Murray, 1996). The normal weight concrete floor, with a total depth of 63.5 mm (2.5 in) on a 25 mm (1.0 in) light gage metal deck, is supported by steel joists and girders. Joist and girder sizes, and bay sizes and shapes are not uniform throughout the floor. In addition, some bays react as a group to floor impacts.

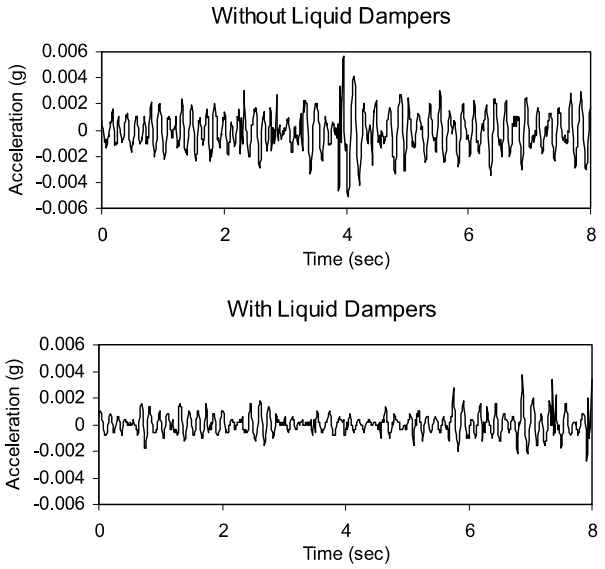

Figure 31. Walking induced response of the building 1 office floor without and with liquid-TMDs

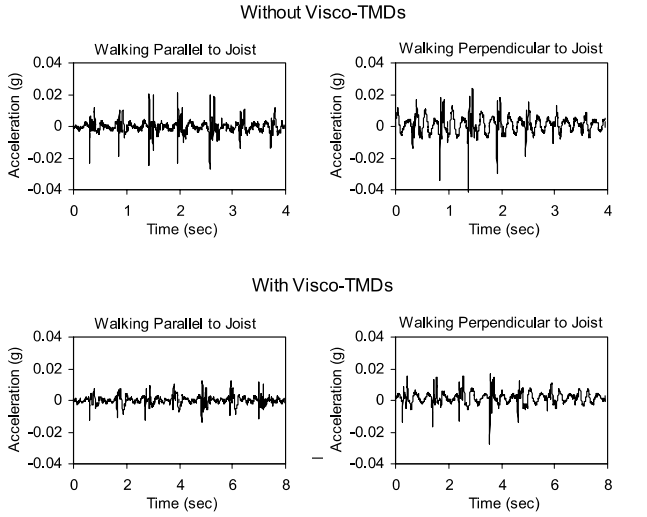

Figure 32. Walking induced response of the building 2 office floor without and with visco-TMDs.

When a stiffer beam or joist did not exist at a column line, the impacts in one bay caused motion in the adjacent bay. Consequently, every bay has a different set of frequencies, and locations of peak amplitudes for specific modes of vibration are not the same for every bay. The non-uniformity of this floor and the impact of adjacent bays result in a very complex vibration response.

The frequencies of the first and second modes of vibration vary for each bay. The different bays of the office floor vibrate at measured frequencies of 4.5–5.5 and 5.5–8 Hz for the first and second modes of vibration, respectively. The spring stiffness, the visco-elastic damping elements, and the mass of the three TMDs described above were modified in an attempt to control specific areas of the office. Tests were conducted in three separate bays of the building.

The first mode of vibration of all the bays was relatively easy to control, since the maximum amplitude for that particular mode of vibration is near the center of the bay. The varying layouts of the floor framing scheme, and size and shapes of the bays made it difficult to determine the location of peak vibration amplitude for the contributing higher modes. Due to cubicle layout, the higher modes of vibration were not as prevalent in some bays as in other bays. When the main walkways were parallel to the joist span, correcting only the first mode of vibration was sufficient; however, when the walkways were perpendicular to the joist span, higher modes contributed significantly to the vibration response. As a result, controlling only the first mode of vibration in these bays was insufficient. The following test results illustrate the difficulties associated with higher modes.

Test results shown in Figure 32 illustrate the effectiveness of the TMDs in a representative bay where only one mode of vibration dominates the vibration response. As noted previously, this condition exists in bays where the walkways are parallel to the joist span. This particular bay is 9.14×12.19 m^2 (30×40 ft^2) with 610 mm deep lightweight steel trusses (24H8 steel joists), spaced at 914 mm (36 in), spanning in the long direction. The dominant mode of vibration had a natural frequency of 5 Hz and maximum amplitude at the center of the bay. Two TMDs were, therefore, configured to control this mode and were placed at the center of the bay.

The test results, noted as walking perpendicular, shown in Figure 32, illustrate the reduced effectiveness of the TMDs in a bay where higher-order modes also contributed significantly to the response. This condition exists in bays where the walkways are perpendicular to the joist span. This bay is 9.14×9.14 m^2 (30×30 ft^2) with 508 mm deep lightweight steel trusses (20H6 steel joists) spaced at 914 mm (36 in) on-center. Two dominant modes of vibration, 5 and 6 Hz, exist in this bay. The controlled response data noted for walking perpendicular to the joists presented in Figure 32 were recorded with one TMD at the center of the bay to control the 5 Hz mode and two TMDs at the edge of the bay to control the maximum amplitude of the 6 Hz mode.

5. Conclusions

Control of floor motion caused by occupant activities is sometimes required because of inadequate design or behavior that was not predicted. Active control has been shown to significantly improve the vibration response of actual floors subjected to occupant excitations. The effectiveness of active control, using an electromagnetic actuator, has been illustrated for both SISO and SIMO schemes. The major drawback of this active system at the present time is the cost of installation. The hardware alone is approximately $16 000 for a single control circuit. We must keep in mind, however, that any new technology is expensive and often becomes more reasonable in time. Maintenance and reliability issues, although not prohibitive, also detract from the attractiveness of an active system.

Two types of TMDs have also been shown to be effective in controlling excessive floor vibrations containing only one significant mode of vibration. Unfortunately, some build-

ing floor systems can be difficult to improve with TMDs because of the presence of multiple complex mode shapes and closely spaced natural frequencies. Another drawback of the TMD is that its effectiveness is limited by the amount of additional mass that can be safely supported by the floor system. For lightly damped floor systems with large amplitudes of resonant or transient vibration, the TMD is an economical and effective repair solution. Research to improve each of these systems continues and will be reported as significant results are achieved.

Acknowledgments

The work discussed by the authors in this paper was supported in part by the National Science Foundation Grants Nos MSS-9201944 and CMS-9503369. Any opinions, findings and conclusions or recommendations expressed in this material are those of the authors and do not necessarily reflect the views of the National Science Foundation. Additional support was provided by a grant from NUCOR Research and Development, Norfolk, Nebraska, and by the 3M Company, St Paul Minnesota. The contributions of graduate research assistants (Ronald L. Shope, Cheryl Rottmann, Saaid M. Saaid, and Ernest C. Kulasekere) are also gratefully acknowledged.

References

Allen, D. E., and Murray, T. M., 1993, "Design Criterion for Walking Vibrations," *Engineering Journal, AISC*, Vol. 31, No. 3, 117–129.

Allen, D. E., 1990, "Building Vibrations from Human Activities," *Concrete International: Design and Construction,* Vol. 12, No. 6, 66–73.

Anderson, B. D., and Moore, J. B., 1990, *Optimal Control – Linear Quadratic Methods*, Prentice-Hall, Englewood Cliffs, NJ.

Balas, M. J., 1979, "Direct Velocity Feedback Control of Large Space Structures," *Journal of Guidance and Control*, Vol. 2, No. 3, 252–253.

Band, B. S., and Murray, T. M., 1996, "Vibration Characteristics of Joist and Joist-Girder Members," *Research Report CE/VPI-ST 96/07*, Department of Civil Engineering, Virginia Polytechnic Institute and State University, Blacksburg, VA.

CSA, 1989, *Steel Structures for Buildings – Limit States Design*, CAN/CSA-S16.1-M89, Canadian Standards Association, Rexdale, Ontario, Canada.

Friedland, B., 1986, *Control System Design: An Introduction to State-Space Systems*, McGraw-Hill, New York.

Franklin, G. F., Powell, J. D., and Emani-Naemi, A., 1986, *Feedback Control of Dynamic Systems*, Addison-Wesley, Menlo Park, CA.

Hanagan, L. M., and Murray, T.M., 1998, "Experimental Implementation of Active Control to Reduce Annoying Floor Vibration," *AISC Engineering Journal*, Vol. 35, No. 4, 123–127.

Hanagan, L. M., and Murray, T. M., 1997, "Active Control Approach for Reducing Floor Vibrations," *Journal of Structural Engineering, ASCE,* Vol. 123, No. 11, 1497–1505.

Hanagan, L. M., Rottmann, C., and Murray, T. M., 1996, "Control of Floor Vibrations," in Proceedings of Structures Congress XIV, Building an International Community of Structural Engineers, S.K. Ghosh and J. Mohammadi, eds., ASCE, New York, 428–435.

Hanagan, L. M., and Murray, T. M., 1995a, "Active Control of Floor Vibration: Implementation Case Studies," in Proceedings of the 1995 American Control Conference Vol. 3, American Automatic Control Council, Department of EECS, Northwestern University, Evanston, IL, 1911–1915.

Hanagan, L. M., and Murray, T. M., 1995b, "Floor Vibration: A New Application for Active Control," in Proceedings of the Fourth Pan American Congress of Applied Mechanics, Universidad del Salvador, Buenos Aires, Argentina, January.

Hanagan, L. M., and Murray, T. M., 1994, "Experimental Results from the Active Control of Floor Motion," in Proceedings of the First World Conference on Structural Control, Vol. 3, 3–5 August 1994, Los Angeles, CA, FP4-71-78.

Hanagan, L. M., 1994, *Active Control of Floor Vibrations,* Ph.D. Dissertation, Technical Report #CE/VPI-ST 94/13, Charles E. Via Department of Civil Engineering, Virginia Polytechnic Institute and State University, Blacksburg, VA.

Inman, D. J., 1994, *Engineering Vibration,* Prentice-Hall, Englewood Cliffs, NJ.

ISO, 1992, "ISO 10137: Basis for the Design of Structures – Serviceability of Buildings Against Vibration," International Standards Organization, 41–43.

Kitterman, S., and Murray, T. M., 1994, "Investigation of Several Aspects of the Vibrational Characteristics of Steel Member Supported Floors," Research Report CE/VPI/ST-94/11, Virginia Polytechnic Institute and State University, Blacksburg, VA.

Lenzen, K. H., 1966, "Vibration of Steel Joist – Concrete Slab Floors," *Engineering Journal, AISC*, Vol. 3, No. 3, 133–136.

Lewis, F. L., 1992, *Applied Optimal Control and Estimation*, Prentice-Hall, Englewood Cliffs, NJ.

MATLAB, 1998, *Control System Toolbox User's Guide*, The Mathworks, Inc., Natick, MA.

McConnel, K. G., 1995, *Vibration Testing: Theory and Practice*, Wiley, New York.

Moerder, D. D., and Calise, A. J., 1985, "Convergence of a Numerical Algorithm for Calculating Optimal Output Feedback Gains," *IEEE Transactions on Automatic Control*, Vol. 30, No. 9, 900–903.

Morley (Hanagan), L. J., and Murray, T. M., 1992, "Predicting Floor Response due to Human Activity," in Proceedings from the International Colloquium for Structural Serviceability of Buildings, Goteborg, Sweden, 297–302.

Murray, T. M., 1991, "Building Floor Vibrations," *Engineering Journal, AISC*, Vol. 28, No. 3, 102–109.

Murray, T. M., 1975, "Design to Prevent Floor Vibrations," *Engineering Journal, AISC*, Vol. 12, No. 3, 82–87.

Murray, T. M., Allen, D. E., and Ungar, E. E., 1997, "Floor Vibrations Due to Human Activity," *AISC Steel Design Guide #11*, AISC, Chicago, IL.

Ogata, K., 1990, *Modern Control Engineering*, Prentice Hall, Englewood Cliffs, NJ.

Pernica, G., 1990, "Dynamic Load Factors for Pedestrian Movements and Rhythmic Exercises," *Canadian Acoustics*, Vol. 18, No. 2, 3–18.

Preumont, A., 2002, *Vibration Control of Active Structures*, Kluwer Academic, Boston, MA.

Reed, F. E., 1988, "Dynamic Vibration Absorbers and Auxiliary Systems," *Shock and Vibration Handbook*, C. Harris, ed., 3rd Ed., Mc-Graw Hill, New York.

Reiher, H., and Meister, F. J., 1931, "The Effect of Vibration on People," (in German), Forchung auf dem Gebeite des Ingenieurwesens, Vol. 2, II, 381 (translation, Report No. F-TS-616-RE H. Q. Air Material Command, Wright Field, OH).

Rottmann, C. E., and Murray, T. M., 1996, "Use of Tuned Mass Dampers to Control Annoying Floor Vibrations," Research Report CE/VPI-ST-96/10, Virginia Polytechnic Institute and State University, Blacksburg, VA.

Rottmann, C., and Murray, T. M., 1997, "The Use of Tuned Mass Dampers to Control Annoying Floor Vibrations," in Applied Mechanics in the Americas, Fifth Pan American Congress of Applied Mechanics, PACAM IV, San Juan, Puerto Rico, 2–4 January, Vol. 3, 416–420.

Saaid, S. M., Hanagan, L. M., and Premaratne, K., 1996, "A Remedy for Excessive Floor Vibration," in Proceedings of the South Florida Section Annual Meeting.

Shope, R., and Murray, T. M., 1995, "Using Tuned Mass Dampers to Eliminate Annoying Floor Vibrations," in Proceedings of Structures Congress XIII, ASCE, Boston, 2–5 Apri, Vol. I, 339–348.

Tedesco, J. W., MacDougal, W. G., and Ross, C. A., 1999, *Structural Dynamics: Theory and Applications*, Addison-Wesley, Menlo Park, CA.

Van de Vegte, J., 1990, *Feedback Control Systems*, Prentice Hall, Englewood Cliffs, NJ.

Wiss, J. F., and Parmelee, R. A., 1974, "Human Perception of Transient Vibrations," *Journal of the Structural Division, ASCE*, Vol. 100(ST4), 773–787.

Wyatt, T. A., 1989, *Design Guide on the Vibration of Floors*, The Steel Construction Institute, Silwood Park, Ascot, UK.

Zimmerman, D. C., and Inman, D. J., 1990, "On the Nature of the Interaction Between Structures and Proof-Mass Actuators," *AIAA Journal of Guidance, Control, and Dynamics*, Vol. 13, No. 1, 82–88.